Asian Journal of Chemistry; Vol. 25, No. 5 (2013), 2821-2828

ASIAN JOURNAL OF CHEMISTRY

www.asianjournalofchemistry.co.in

Simplified Simultaneous Determination of Concentrations of V^{2+}, V^{3+} and V^{4+}: An Example of Inverse Problems

H.Y. Li[1,2], T. Yamamura[3], S. Ohta[3], C. Gao[1], X.J. Xiang[2], Y.F. Xia[1], J.W. Liu[1], S.Q. Liu[1], D.X. Li[3], M. Jin[2], K.C. Zhou[1,*] and X.W. Wu[1,2,3]

[1]School of Chemistry and Chemical Engineering, State Key Laboratory of Powder Metallurgy, Central South University, Changsha 410083, Hunan Province, P.R. China
[2]School of Science, Hunan Agricultural University, Changsha 410128, Hunan Province, P.R. China
[3]Institute for Materials Research, Tohoku University, Sendai, Miyagi 980-8577, Japan

*Corresponding author: Fax: +86 731 8879616; Tel: +86 731 8879850; E-mail:zhoukc2@mail.csu.edu.cn

(*Received*: 3 May 2012; *Accepted*: 23 November 2012) AJC-12461

A simplified spectrophotometric method was developed for the simultaneous determination of concentrations (c_n) of vanadium ions at different oxidation states, which has applications in vanadium redox-flow batteries. This method is of particular use for mixed V^{3+}/VO^{2+} and V^{2+}/V^{3+} solutions. A singular value decomposition was applied to the spectra to resolve the severe overlaps of the spectra of these cations and to obtain the selected wavelength λ^k. By using absorbance obtained at the selected wavelength in the single- and mixed-valence solutions, the coefficient matrices G = {g_k, n} were determined *via* the least squares method. The determined formulae are: $C_n = \sum_{k=1}^{n} gk, nI_k$, where I_k is the absorbance at λ^1 = 520 nm, λ^2 = 401 nm, λ^3 = 770 nm, or λ^4 = 320 nm. The determined concentrations agree well (within 5 %) with those determined using other methods.

Key Words: Spectrophotometry, Singular value decomposition, Least-squares method, Vanadium Redox-flow battery.

INTRODUCTION

The vanadium redox-flow battery uses vanadium cations of four oxidation states: V^{2+} and V^{3+} in the negative electrolyte and VO^{2+} and VO_2^+ in the positive electrolyte[1,2]. The unique advantages of the battery, including long cycle life, deep-discharge capacity, flexible operation and its large scale[3,4], have encouraged its adoption, as seen in the Tomamae plant in Japan (450 kW and 4 MW/6 MWh class system)[5]. In the course of the R & D of the vanadium redox-flow battery, a strong demand has developed for the simultaneous quantitative determination of the four vanadium cations in a manner that is convenient for a large number of samples[6,7].

Quantitative analysis of part of the four vanadium cations has been conducted using extractants, oxidants, or flow columns, but no simultaneous determination has occurred. The quantitative analysis of vanadium has focused on vanadium(V) and vanadium(IV) using various spectrophotometric methods with extractants or complexing reagents[8]. The simultaneous determination of the concentrations of VO_2^+ and VO^{2+} has been investigated using the spectrophotometric flow injection method with complexing agents[9,10]. The concentration of VO^{2+} has been determined using redox titration to VO_2^+ with $KMnO_4$[11]. However, for the *in situ* determination of vanadium concentrations in the electrolytes of the vanadium redox-flow battery, a simple method should be developed using ultraviolet spectrophotometry[12].

The electrolytes of the vanadium redox-flow battery have unique features which enable us to use the simultaneous spectrophotometric method. First, all of the four cations have unique spectra with (V^{2+}, V^{3+} and VO^{2+}) or without (VO_2^+) multiple peaks at different wavelengths (Fig. 1). $V^{2+}(3d^3)$ and $V^{3+}(3d^2)$ have spin-allowed and Laporte forbidden transitions with relatively large absorption (molar absorption coefficient ε = *ca.* 20) in the visible region. The absorptions of $V^{2+}[^4A_{2g}(4F)]$ have been observed at 850 nm [$\rightarrow$ $^4T_{2g}(4F)$], 560 nm [$\rightarrow$ $^4T_{1g}(4F)$] and 370 nm [$\rightarrow ^4T_{1g}(4P)$][13]. Similarly, the absorptions of V^{3+} [$^3T_{1g}(3F)$] have been observed at 605 nm [$\rightarrow$ $^3T_{2g}(3F)$] and 400 nm ($\rightarrow$ $^3T_{1g}(3P)$)[14]. The absorptions of $VO^{2+}(3d^1, b^1_2)$ have been ascribed to transitions between molecular orbitals $e\pi^*$ at 760 nm and b^*_{1g} at 620 nm[15]. A closed shell $VO_2^+(3d^04s^0)$ has no transition in the visible region, but has a strong MLCT shoulder in the ultraviolet region. Second, the concentrations of the total vanadium ions are as great as 1-4 mol dm^{-3} for vanadium redox-flow battery applications. This provides the appropriate conditions for spectrophotometric detection (absorbance should be in the order of 0.1-2) with a possible dilution if necessary. Third, the total concentration of the vanadium ions are usually known for vanadium redox-flow battery applications and thus may eliminate one unknown parameter in the equations. This is because all of the four oxidation states can be mutually transformed by electrolysis as[16]:

$$V^{3+} + e^- \rightleftharpoons V^{2+}\ (E^0\ V^{3+}/V^{2+} = -0.255\ V) \quad (1)$$

$$VO^{2+} + 2H^+ + e^- \rightleftharpoons V^{3+} + H_2O\ (E^0\ VO^{2+}/V^{3+} = 0.337\ V) \quad (2)$$

$$VO_2^+ + 2H^+ + e^- \rightleftharpoons VO^{2+} + H_2O\ (E^0\ VO_2^+/VO^{2+} = 1.000V) \quad (3)$$

In this study, we present the simplest simultaneous determination of concentrations of V^{2+}, V^{3+}, VO^{2+} and VO_2^+. The method used is the least-squares regression of the multiple variables. It is neither principal component analysis nor principal component regression[17]. The difficulty in the decomposition of the four spectra lies in the severe overlap without orthogonal transformation. To extract the wavelength characteristics of the cations and the corresponding coefficients, the pseudo-inverse matrix of the absorption matrix was checked and base vectors were generated by the singular value decomposition of the absorption coefficient matrix. After determining the wavelengths and the coefficients, the method was checked for applicability to several solutions. The method is especially effective for the mixed V^{3+}/VO^{2+} and V^{2+}/V^{3+} solutions and will therefore have wide practical applications for operating and monitoring vanadium redox-flow batteries.

THEORY

Absorption spectrum of the mixture of vanadium cations: At a wavelength of mth region (m = 1, 2, ..., M), a certain chemical species *n* may have a molar absorption coefficient $\Lambda_{m,n}$. For the species, the molar absorption coefficients for a unit concentration (1 mol dm^{-3}) and a unit path length (1 cm) are given by $a_n = \{\Lambda_{m,n}\}$, where $\Lambda_{m,n}$ ($dm^3\ mol^{-1}\ cm^{-1}$) is the absorption coefficient. Consider the absorption spectrum of the mixture. The concentrations of V^{2+}, V^{3+}, VO^{2+} and VO_2^+ are defined as c_1, c_2, c_3 and c_4, respectively. The ascending order of the redox potentials in reactions (1)-(3) as $E^0_{V^{3+}/V^{2+}} < E^0_{VO^{2+}/V^{3+}} < E^0_{VO_2^+/VO^{2+}}$ imposes a strict limit on the four cations. In this study, the quantitative analysis focused on V^{2+}, V^{3+} and VO^{2+}. Thus, four cases were selected, as described later. This leads to a contraction of the system from M to a number as large as the number of species. The absorption spectrum, $y_n = \{I_{m,n}\}$, of the species n(n = 1 for V^{2+}, 2 for V^{3+}, 3 for VO^{2+}, 4 for VO_2^+) with a concentration c_n for a fixed path length of 1 cm is given by Lambert-Beer's law as:

$$y_n = c_n \Lambda_n \quad (4)$$

If chemical interactions between species are negligible, the absorption spectrum of the mixture of N-species ($N = N_2 - N_1 + 1$) is obtained by the sum of eqn. (4):

$$y = \sum_{n=N_1}^{N_2} c_n a_n = AC \quad (5)$$

Here, we define the absorption coefficient matrix $A = (\Lambda_1 \cdot \cdot \cdot \Lambda_N)$ and the concentration vector $c = \{c_n\}$. Equation (5) is for the linear system, where the absorption spectrum y is connected to the concentrations of the species c through the absorption coefficient matrix A. This means that the concentrations c are easily deduced from the absorption spectra y.

Solution of concentration vector using the least-squares method: Because the measured spectrum y includes errors e = {em} (m = 1, · · ·, M), eqn. (5) is given by:

$$y = Ac + e \quad (6)$$

The minimum value of the squared error can be obtained as follows:

$$Q(c) = e^Te = (y-Ac)^T(y-Ac) \quad (7)$$

By letting $\Lambda Q/\Lambda c = 0$, we obtain the regular equation:

$$A^TAc = A^Ty \quad (8)$$

If A^TA are the regular matrix ($\det A^TA \neq 0$), the matrix can be transformed by determining the analyzed concentration vector $\hat{c}$:

$$\hat{C} = (A^TA)^{-1}A^Ty \quad (9)$$

$$= \quad Fy \quad (10)$$

Solution of the inverse problem (10): Equation (6) shows that a very large vector y with a dimension of M × 1 is required to determine the small vector c with a dimension of N × 1. However, it is expected that rank A=N, which can be understood from the number of the different vectors ($a_1, \cdot \cdot \cdot, a_N$). This means that the matrix A can be decomposed into a M × k matrix $U = (u_1 \cdot \cdot \cdot u_k)$ and k × k matrix $V = (v_1 \cdot \cdot \cdot v_k)$ using singular value decomposition:

$$A = U\ DV^T$$

Here, k is the number of the eigen values and the eigenvectors and is possibly equal to N. These vectors U and V are orthonormal matrices and the vector $D = \mathrm{diag}\{\gamma_k\}$ (k = 1, · · ·, 4) is the diagonal matrix with singular values γ_k. Because vector U and V are orthonormal matrices, the singular values, γ_k, correspond to the molar absorption coefficients, $a_{m,n}$. The vector F in Eq. (10) can also be decomposed by singular value decomposition and can be rewritten as:

$$F = VD^{-1}\ U^T \quad (12)$$

This leads us to the transformation of Eq. (10):

$$V^T\hat{c} = D^{-1}U^Ty \quad (13)$$

Equation (13) is equivalent to the equations: $c = \sum_{k=1}^{4} a_k \nu_k$ and $y = \sum_{k=1}^{4} \beta_k u_k$, where

$$\alpha_k \gamma_k = \beta_k \quad (14)$$

If the submatrix $B = (b_1 \cdot \cdot \cdot b_P)$ with minimum P can be determined, z, which is a submatrix of y, yields c. This occurs, for instance, in the system in which four different cations V^{2+}, V^{3+}, VO^{2+} and VO_2^+ are included (as in **Case 4** in Table-2). We define the submatrices b_n and z as:

$$b_n = [a_p, n, a_q, n, a_r, n, a_s, n]^T \quad (15)$$

$$z = [I_p, I_q, I_r, I_s]^T \quad (16)$$

$$= \{I\lambda_n k\}\ (k = 1, \cdot \cdot \cdot, 4) \quad (17)$$

where $1 \leq p < q < r < s \leq M$. Here, we obtain

$$z = Bc$$

For the simplified calculation, where N × N matrix B for a characteristic wavelength ($\lambda_1, \cdot \cdot \cdot, \lambda_N$), Eq. (18) can be used. If b_n are all vertical, rank A = 4 is true. However, as shown in Fig. 1, n-b_n are not perpendicular to each other. Therefore, $[\alpha, 0, 0, 0]^T$, $[0, \beta, 0, 0]^T$, · · · with p, q, r, s cannot be chosen.

EXPERIMENTAL

Oxovanadium(IV) sulfate ($VOSO_4 \cdot nH_2O$) was purchased from Wako Pure Chemical Industries Ltd., Japan. All reagents were used as purchased. Doubly distilled water obtained from a 1810D (SENCO, China) was used during the experiments. The absorption spectrophotometer in the visible and ultraviolet region, UV-3100PC (Shimadzu Corp., Kyoto, Japan) was used with a quartz optical cell with a path length of 1 cm. An ICP atomic emission spectrometer, ICPS-7500 (Shimadzu Corp., Kyoto, Japan) was used to determine the total vanadium concentration.

Preparation of the standard solution: The H_2SO_4 solutions were first degassed through Ar gas bubbling. The preparation of the sulfuric solutions of V^{2+}, V^{3+}, VO^{2+} and VO_2^+ were carried out using methods similar to those described in our previous work[18]. A solution of $VOSO_4$(2 mol dm^{-3}, 50 mL) in aqueous sulfuric acid (2 mol dm^{-3}) was electrochemically reduced on a mercury cathode under a constant current of 1 A using a galvanostat (HA-501, Hokuto Denko Co. Ltd., Japan). The V^{2+} solution was used when freshly prepared and its final concentration was determined to be 1.431 mol dm^{-3} using ICP. The aqueous solution was exposed to air overnight and then the excess sulfuric acid was removed *via* evaporation for a few days to prepare the $V(SO_4)_{1.5} \cdot x_3H_2O$ solid ($x_3 = 8.15$). The pentavalent salt $VO_2(SO_4)_{0.5} \cdot x_5H_2O$ and divalent salt $VSO_4 \cdot x_2H_2O$ were prepared using electrolytic oxidation of the tetravalent salt and electrolytic reduction from the trivalent salt, respectively. These solid salts were dissolved in 2 mol dm^{-3} H_2SO_4. For the V^{2+}, VO^{2+} and VO_2^+ standard solutions, 100 mL of the stock (0.1 mol dm^{-3}) vanadium solution was prepared by dissolving $V(SO_4)_{1.5} \cdot 8.15H_2O$, $VOSO_4 \cdot 3.7H_2O$ and $VO_2(SO_4)_{0.5} \cdot x_5H_2O$, respectively, in doubly distilled de-ionized water containing 10 mL of sulfuric acid (1+1). To prepare the calibration curves of V^{2+}, V^{3+} and VO^{2+} solutions, 2 mol dm^{-3} H_2SO_4 solutions with known concentrations of vanadium were prepared: $[V^{2+}]$ = 0.0283, 0.0565, 0.0848, 0.113, 0.141 and 0.170 mol dm^{-3}; $[V^{3+}]$ = 0.004, 0.006, 0.008, 0.010, 0.020, 0.024, 0.028, 0.032, 0.036 and 0.040 mol dm^{-3}; $[VO^{2+}]$ = 0.004, 0.008, 0.012, 0.016, 0.020, 0.040 and 0.060 mol dm^{-3}.

RESULTS AND DISCUSSION

Molar absorption coefficient matrices for V^{2+}, V^{3+}, VO^{2+} and VO_2^+. The absorption spectra were recorded over 300-950 nm against a blank solution. The molar absorption coefficients $a_n = \{a_{m,n}\}$($dm^3mol^{-1}cm^{-1}$) (m = 1, · · ·, M) are the obtained spectra of V^{2+}, V^{3+}, VO^{2+} and VO_2^+ in sulfuric acid solutions over the region spanning from 300 to 950 nm with a resolution of 1 nm (M = 651, Fig. 1). The absorption peaks were located at about 520 nm (V^{2+}), 401 nm (V^{3+}), 610 nm (V^{3+}) and 770 nm (VO^{2+}) (Table-1).

Case combinations: Possible coexistence of vanadium ions in a solution. For the first step, the nature of the reversed transformation of y^c is investigated by checking the pseudo-inverse of A = ($a_1a_2a_3a_4$) defined as:

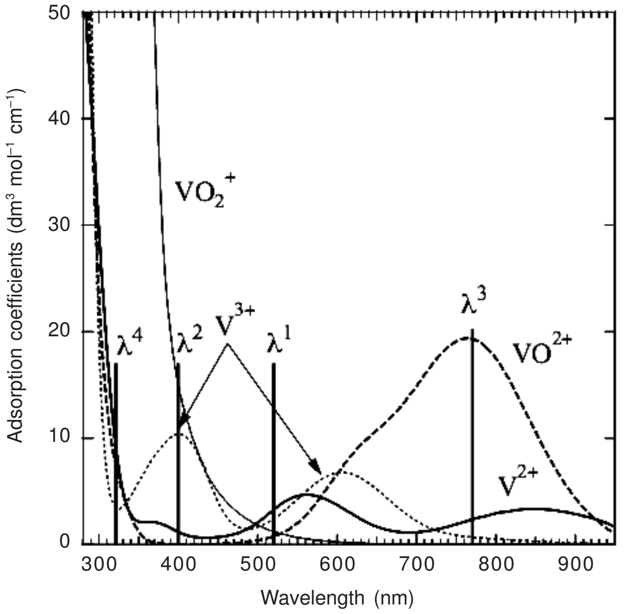

Fig. 1. Absorption coefficients of V^{2+}, V^{3+}, VO^{2+}, VO_2^+ *versus* wavelength. See text for vertical bars indicating λ_k(k = 1,…,4)

TABLE-1
MOLAR ABSORPTION COEFFICIENT (a_n) ON SPECIFIC ABSORPTION POSITIONS

n	V cation	a_n[a](λ n/nm)	Reported values of a_n[a](λ n/nm)
1	V^{2+}	3.12(520)	3.1(359), 6.0(540), 4.1(842)[b]
2	V^{3+}	11.7(401), 7.25(610)	6.6(389), 3.5(562)[c]
3	VO^{2+}	18.4(770)	18(750)[d]
4	VO_2^+	n.d. [e]	n.d.[e]

a) Molar absorption coefficient/dm^3 mol^{-1} cm^{-1}; b) Solid of $VSO_4 \cdot 7H_2O$ in ref.[13]; c) Solid of $NH_4V(SO_4)_2 \cdot 12H_2O$ in ref.[19]; d)VO^{2+} in 8 mol dm^{-3} H_2SO_4 in ref.[20]; e) VO_2^+ has no peak owing to transition in the visible region

$$F = (A^TA)^{-1}A^T \tag{19}$$

As expected, the content of F depends on how the combination of a_n is selected. From the standard potentials shown in reactions (1)-(3), only six combinations are possible in identical solutions. Among them, four combinations of vanadium cations are considered in this study. **Case 1** includes V^{2+} and V^{3+}, which can be applied to the quantification analysis of the negative electrolyte solution of vanadium redox-flow battery. **Case 2** contains V^{2+}, V^{3+} and VO^{2+}. These three cations can exist in an identical solution, as expected from the standard potentials shown in reactions (1) and (2). If the total vanadium concentration is known, **Case 2** can be applied to all types of solutions, even those including VO_2^+. Furthermore, spectroscopic decomposition in **Case 2** may be the most difficult and thus the case can be used as an indicator of the successfulness of this method. **Case 3** includes V^{3+} and VO^{2+} ions. This case is typically applicable to vanadium solutions that remain open to air. **Case 4** contains all of the cations: V^{2+}, V^{3+}, VO^{2+} and VO_2^+.

The reversed transformation coefficients $f_n = \{f_{m,n}\}$(dm^3 mol^{-1}) are shown along with the wavelength in Figs. 2 and 3. The pseudo-inverse spectra show the contribution of absorption intensity at a certain wavelength to the concentration of a certain cation. The figure demonstrates that the reversed transformation coefficients differ depending on the case combinations, however, selecting the characteristic wavelength is still difficult because of two major problems. First, no information is available in the non-base vector used here (*f*) about how many and which combination of selected wavelengths are required for quantification with rationally small errors. Second, for example, the VO_2^+ coefficients in **Case 4** are too small compared with those of other ions.

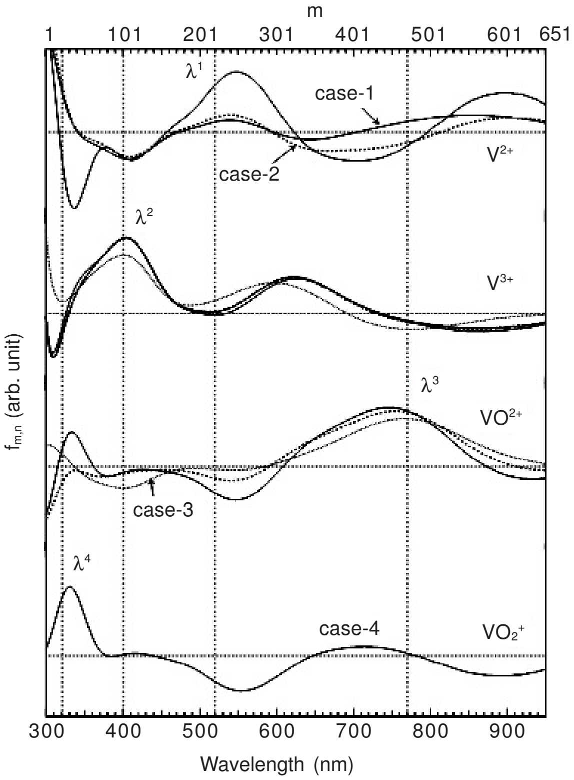

Fig. 2. Pseudo-inverse spectra of V^{2+}, V^{3+}, VO^{2+} and VO_2^+ for various combinations of vanadium ions. See text for vertical bars indicating λ_k(k = 1,…, 4)

Eigenvectors of the spectra and concentrations: We determined eigenvectors ν_k corresponding to the eigen-values γ_k for the whole spectra (M = 651) (Table-2). The corresponding eigenvectors u_k are shown in Fig. 4. The matrix F was successfully decomposed into two (**Cases 1** and **3**), three (**Case 2**) and four (**Case 4**) unique eigenvectors. Eigenvectors are base vectors with unit magnitude, meaning that each vector is perpendicular to any other. The nature of the base vector provides a guide for selecting the sampling wavelength. It is noted that the vector may be similar to the spectrum of the real ion, but it may also be a linear combination of multiple spectra. In **Case 1**, each vector was decomposed into the contribution from each valence ion. For instance, in **Case 4**, ν_1 was mainly composed of n = 4 (VO_2^+) and ν_4 of n = 1 (V^{2+}). However, the vectors ν_2 and ν_3 had similar major contributions from both n = 3 (VO^{2+}) and n = 2 (V^{3+}). It is noted that n = 3(VO^{2+}) and n = 2 (V^{3+}) components made equal contributions to both ν_1 and ν_2, with minus-minus and minus-plus linear combinations to these vectors. This close relationship between V^{3+} and VO^{2+} can be attributed to the spectral overlap near 600 nm. In contrast, vectors ν_k in **Cases 1, 2** and **3** had major contribution from all of the components.

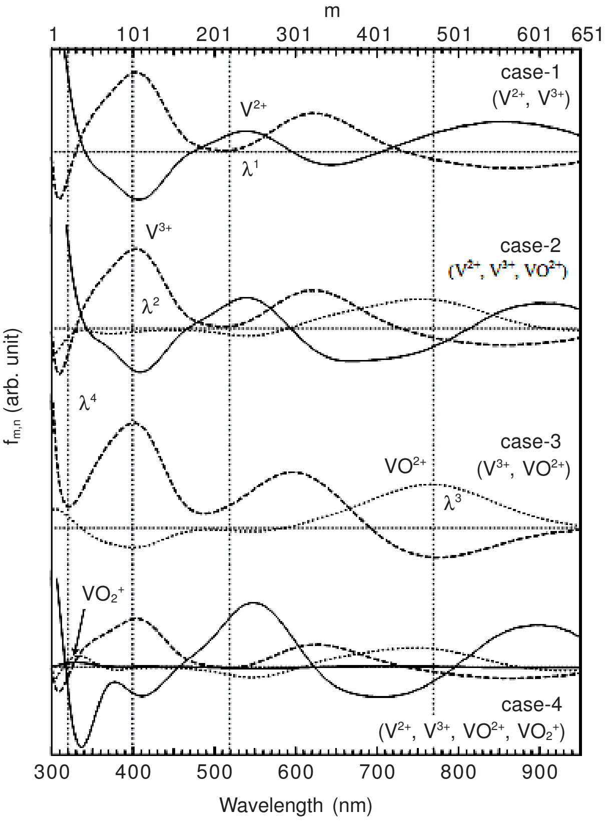

Fig. 3. Pseudo-inverse spectra of V^{2+}, V^{3+}, VO^{2+} and VO_2^+. Reorganized for various combinations of vanadium ions. See text for vertical bars indicating λ_k(k = 1,…, 4)

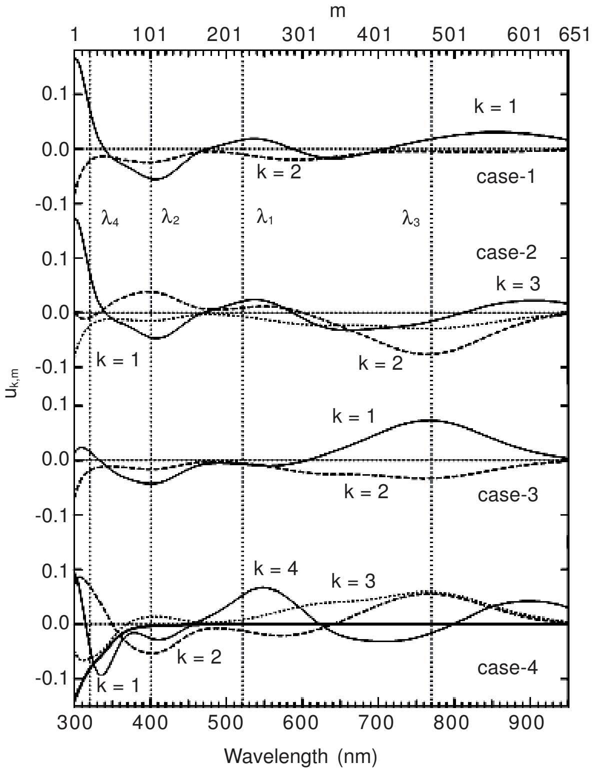

Fig. 4. u_k for 1 to 4. See text for vertical bars indicating λ_k (k = 1,…, 4)

TABLE-2
EIGENVECTORS ν_k CORRESPONDING TO THE EIGEN VALUES γ_k FOR THE WHOLE SPECTRA (M = 651). FOR CORRESPONDING EIGENVECTORS u_k, (Fig. 4)

Case [a]	k	$u_k/10^3$	ν_k
1	1	0.385	(-0.548 -0.836)
	2	0.086	(0.836 -0.548)
2	1	0.482	(-0.433 -0.628 -0.647)
	2	0.179	(0.192 0.637 -0.746)
	3	0.080	(0.881 -0.447 -0.155)
3	1	0.436	(-0.686 -0.728)
	2	0.176	(-0.728 0.686)
4	1	4.20	(-0.049 -0.062 -0.051 -0.996)
	2	0.293	(0.225 0.469 0.850 -0.084)
	3	0.160	(-0.090 -0.860 0.502 0.032)
	4	0.049	(0.969 -0.192 -0.153 -0.028)

a) **Case 1**: V^{2+} and V^{3+}; **Case 2**: V^{2+} and V^{3+} and VO^{2+}; **Case 3**: V^{3+} and VO^{2+}; **Case 4**: V^{2+} and V^{3+} and VO^{2+} and VO_2^+

Calibration of contracted absorbance matrix in single valence solutions: For the experiments with the number of samples S, we obtain the concentration matrix: $C = (c_1 \cdots c_S)$ and the absorbance matrix $Z = (z_1 \cdots z_S)$. Our problem is given by: $Z = BC$, or $C = GZ$. Here, the matrix G is described by B and then decomposed using singular value decomposition:

$$G = (B^TB)^{-1}B^T \quad (21)$$

$$= V_bD_b^{-1}U_b^T \quad (22)$$

In the contracted treatment, the contracted transformation matrix G was successfully decomposed into N components. To decompose the matrix G into N components, the sampling wavelength must be selected to detect the differences in u_k from other components.

Sampling wavelengths λ^k were selected as 520 nm (k = 1), 401 nm (k = 2), 770 nm (k = 3) and 320 nm (k = 4) by choosing the wavelengths at which the magnitudes are almost at a maximum in Fig. 4. The selection of these wavelengths can be understood by the large contribution of V^{2+}, V^{3+}, VO^{2+} and VO_2^+, respectively, in Fig. 2.

Fig. 5 summarizes the calibration curves for V^{2+}, V^{3+} and VO_2^+ at several selected wavelengths. Excellent linearities were observed for all of these wavelengths. The slopes of the lines in Fig. 5 correspond to the molar absorption coefficients of the vanadium cations at the wavelengths. The values of V^{2+} at 520 nm, V^{3+} at 401 nm and VO^{2+} at 770 nm were 3.12 (reciprocal value 0.321), 11.7 (0.086) and 18.4 (0.054), respectively.

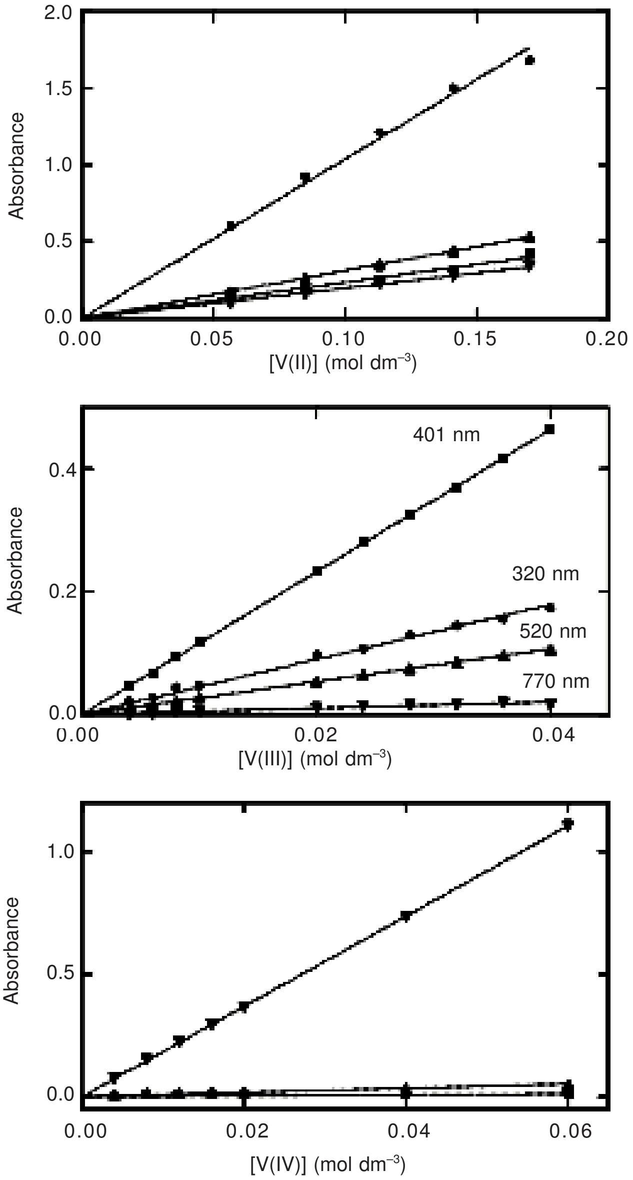

Fig. 5. Calibration curves of V^{2+}, V^{3+}, and VO^{2+} (●; 320 nm, ■; 401 nm, ▲; 520 nm, ▼; 770 nm)

The eigenvectors u_k and ν_k that correspond to the eigenvalues γ_k for the contracted matrices (M = 4) are summarized in Table-3. The eigenvectors ν_k (k = 1 ··· 4) are mainly contributed from k = n and the eigenvalue γ_k is similar to the reciprocal of the molar absorption coefficients, because the matrices Z with contracted size (M = 4) are generated by sampling absorption intensity at selected wavelengths (λ^k), where k = n. For example, in **Case 1**, ν_1 is mainly composed from the component n = 1 and ν_2 is composed from that of n = 2. In Table-3, for k = 2 in **Case 1** and **Case 2** and k = 1 in **Case 3**, u_k^{-1} values are shown to be about 0.08. This value is the same as the reciprocal value of the molar absorption coefficient in V^{3+}. It is shown that this component is mainly V^{3+}. For k = 3 in **Case 2** and k = 2 in **Case 3**, this component is mainly VO^{2+}.

By contrast, for k = 1 in **Case 1** and **Case 2**, u_k^{-1} are shown to have large values compared with the reciprocal value of the molar absorption coefficient in V^{2+}. This causes the absorption spectrum (Fig. 1) in 520 nm, in which this wavelength is selected for V^{2+}, to show similar values to V^{2+} and V^{3+}.

TABLE-3
EIGENVECTORS $(u_k^b)^T$ AND v_k CORRESPONDING TO THE EIGENVALUES u_k^{-1} FOR THE CONTRACTED MATRICES (M = 4) DETERMINED FOR (a) ONLY SINGLE-VALENCE SOLUTIONS AND FOR (b) ALL SOLUTIONS, INCLUDING MIXED-VALENCE SYSTEMS

Case[a)]	k	Single-valence solution			Mixed-valence solution		
		u_k^{-1}	v_k	u_k^{bT}	u_k^{-1}	v_k	u_k^{bT}
1	1	0.410	(-0.962 0.272)	(-0.968 0.252)	0.409	(-0.966 0.259)	(-0.969 0.246)
	2	0.081	(0.272 0.962)	(0.252 0.968)	0.077	(0.259 0.966)	(0.246 0.969)
2	1	0.427	(-0.962 0.267 0.057)	(-0.964 0.246 0.104)	0.429	(-0.964 0.260 0.058)	(-0.963 0.250 0.106)
	2	0.082	(-0.260 -0.960 0.100)	(-0.234 -0.965 0.117)	0.078	(-0.256 -0.964 0.075)	-0.240 - 0.966 0.095)
	3	0.054	(0.081 0.081 0.992)	(0.129 0.088 0.988)	0.054	(0.075 0.057 0.996)	0.126 0.066 0.990)
3	1	0.086	(-0.999 0.044)	(-0.999 0.055)	0.086	(-0.999 0.033)	-0.999 0.042)
	2	0.054	(0.044 0.999)	(0.055 0.999)	0.055	(0.033 0.999)	0.042 0.999)
	1	-	-	-	0.416	(-0.964 0.259 0.064 -0.009)	-0.968 0.225 0.108 0.002)
	2	-	-	-	0.079	(-0.259 -0.965 0.015 0.039)	-0.221 -0.974 0.054 0.002)
	3	-	-	-	0.055	(-0.064 0.001 -0.998 0.001)	-0.117 -0.029 -0.993 0.002)
	4	-	-	-	0.000	(0.002 0.040 0.001 0.999)	0.003 0.001 0.002 1.000)

a) **Case 1**: V^{2+} and V^{3+}; **Case 2**: V^{2+}, V^{3+} and VO^{2+}; **Case 3**: V^{3+} and VO^{2+}; **Case 4**: V^{2+}, V^{3+}, VO^{2+} and VO_2^+; b) The calculations for only mixed-valence solution

Quantitative analysis in mixed-valence solutions: The matrices of F were first calculated from absorption spectra of single-valence solutions. Then, the matrices F were calculated by including mixed-valence solutions, which are shown in Figs. 6-8. In both solutions, we sampled data with or without mixed-valence solutions; the components of F are summarized in Table-4. To assess the first question, which arose earlier, eight sets of selected wavelengths were tested for all of the test solutions used in this study. We list the deviations of the calculated concentrations of c_n using f_n, which is calculated by changing the selected wavelength in Table-5. Although the precision of the calculated concentration is almost unchanged when one of the selected wavelengths (Set 1-3) is changed, it is enhanced when the selected wavelength (Set 5-8) is changed in **Case 1**.

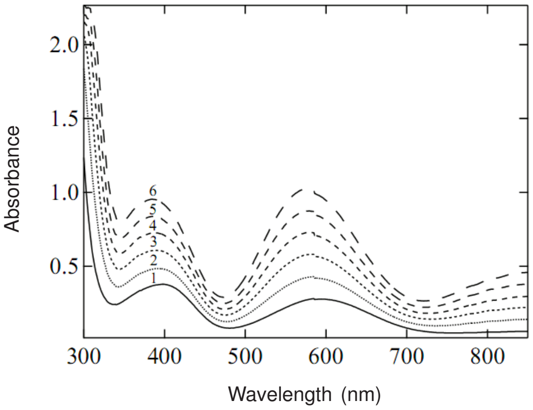

Fig. 6. Absorption spectra of mixed solutions of V^{2+} and V^{3+} in 2 mol dm^{-3} H_2SO_4. Concentrations (mol dm^{-3}) of V^{2+} and V^{3+} were 0.0283 and 0.0200 for solution No. 1, 0.0565 and 0.0240 for No. 2, 0.0849 and 0.0280 for No. 3,0.1130 and 0.0320 for No. 4, 0.1410 and 0.0360 for No. 5 and 0.1700 and 0.0400 for No. 6

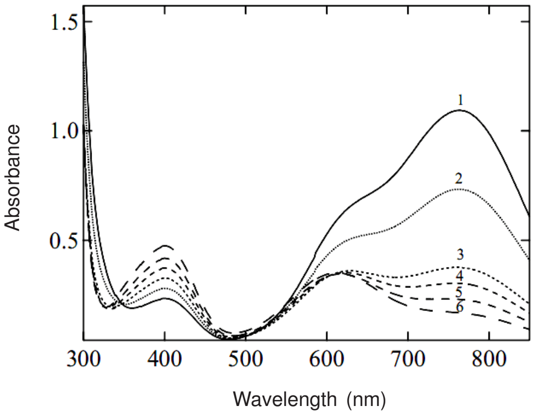

Fig. 7. Absorption spectra of mixed solutions of V^{3+} and VO^{2+} in 2 mol dm^{-3} H_2SO_4 Concentrations (mol dm^{-3}) of V^{3+} and VO^{2+} were 0.020 and 0.060 for solution No. 1, 0.024 and 0.040 for No. 2, 0.028 and 0.020 for No. 3, 0.032 and 0.016 for No. 4, 0.036 and 0.012 for No. 5 and 0.040 and 0.008 for No. 6

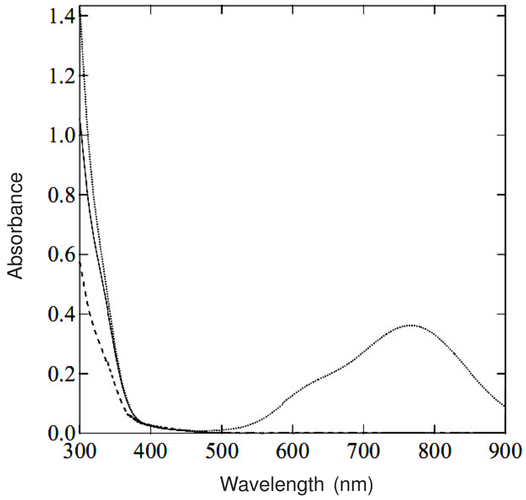

Fig. 8. Absorption spectra of solutions of VO_2^+ and VO^{2+} in 2 mol dm^{-3} H_2SO_4

TABLE-4
REVERSED TRANSFORMATION COEFFICIENTS g^k_n FOR nth SPECIES AT SELECTED WAVELENGTHS u_k (/nm) FOR MIXED-VALENCE SOLUTIONS

Set[a)]	Case[b)]	n[c)]	g^k_n at selected wavelength (/nm)				
			λ' (610)	$λ^1$ (520)	$λ^2$ (401)	$λ^3$ (770)	$λ^4$ (320)
0	1	1	-	3.88×10^{-1}	-8.46×10^{-2}	-	-
		2	-	-7.76×10^{-2}	9.79×10^{-2}	-	-
	2	1	-	4.03×10^{-1}	-8.89×10^{-2}	-1.84×10^{-2}	-
		2	-	-8.36×10^{-2}	1.01×10^{-1}	4.07×10^{-3}	-
		3	-	-4.16×10^{-2}	7.74×10^{-3}	5.67×10^{-2}	-
	3	1	-	-	8.60×10^{-2}	-4.99×10^{-4}	-
		2	-	-	-1.83×10^{-3}	5.49×10^{-2}	-
	4	1	-	3.93×10^{-1}	-8.76×10^{-2}	-1.89×10^{-2}	2.88×10^{-3}
		2	-	-7.04×10^{-2}	9.86×10^{-2}	6.22×10^{-3}	-3.86×10^{-3}
		3	-	-4.07×10^{-2}	7.39×10^{-3}	5.73×10^{-2}	-2.60×10^{-4}
		4	-	-9.88×10^{-4}	1.40×10^{-4}	-6.97×10^{-5}	2.87×10^{-3}
5	1	1	-9.63×10^{-1}	1.14	3.32×10^{-1}	-	-
		2	1.14	-9.67×10^{-1}	-3.96×10^{-1}	-	-
	2	1	1.45×10^{-2}	-3.96×10^{-1}	-9.60×10^{-2}	-2.39×10^{-2}	-
		2	3.72×10^{-1}	-2.68×10^{-1}	-7.95×10^{-2}	-1.37×10^{-1}	-
		3	4.55×10^{-2}	-6.42×10^{-2}	-1.43×10^{-2}	3.94×10^{-2}	-
	3	2	1.31×10^{-1}	-	7.12×10^{-3}	-5.32×10^{-2}	-
		3	1.42×10^{-1}	-	-8.74×10^{-2}	2.23×10^{-3}	-
	4	1	-4.95×10^{-3}	3.96×10^{-1}	-8.52×10^{-2}	-1.70×10^{-2}	2.84×10^{-3}
		2	2.59×10^{-2}	-8.38×10^{-2}	8.61×10^{-2}	-3.78×10^{-3}	-3.67×10^{-3}
		3	-2.73×10^{-3}	-3.93×10^{-2}	8.70×10^{-3}	5.83×10^{-2}	-2.80×10^{-4}
		4	-5.57×10^{-4}	6.98×10^{-4}	4.08×10^{-4}	1.45×10^{-4}	2.83×10^{-4}

a) The values for set 1-4 and 6-8 were omitted here. Refer to Table-5; b) **Case 1**: V^{2+} and V^{3+}; **Case 2**: V^{2+}, V^{3+} and VO^{2+}; **Case 3**: V^{3+} and VO^{2+}; **Case 4**: V^{2+}, V^{3+}, VO^{2+} and VO_2^+; c) n corresponds to vanadium cation as: V^{2+} (n = 1), V^{3+} (n = 2), VO^{2+} (n = 3) and VO_2^+ (n = 4)

TABLE-5
EXTENT OF DEVIATION[h)](/%) FOR THE CALCULATED CONCENTRATIONS OF c_n USING g_n CALCULATED BY CHANGING THE SELECTED WAVELENGTH

Selected wavelength[g)]/nm					Case[i)]	Single-valence solution		Mixed-valence solution[b)]	
Set	$λ^1$	$λ^2$	$λ^3$	$λ^{j)}$		C1[c)]	C2[d)]	C1[c)]	C1[e)]
0	520	401	470	-	1	-8 ~ -2	-8 ~ -6	-5 ~ 0	-1 ~ 17
					2	-8 ~ 3	-5 ~ -4	-5 ~ 0	0 ~ 19
1	850	401	770	-	1	-12 ~ 3	-8 ~ -6	-8 ~ 0	-1 ~ 18
					2	-10 ~ 3	-6 ~ -4	-7 ~ 0	0 - 19
2	520	610	770	-	1	-7 ~ 2	-7 ~ -4	-4 ~ 0	0 ~ 14
					2	-8 ~ 2	-5 ~ -4	-5 ~ 0	0 ~ 17
3	550	401	770	-	1	-8 ~ 3	-8 ~ -6	-6 ~ 0	-1 ~ 17
					2	-7 ~ 3	-6 ~ -4	-7 ~ 0	0 ~ 19
4	850	610	770	-	1	-12 ~ 3	-9 ~ -6	-8 ~ 0	-1 ~ 18
					2	-25 ~ 3	-29 ~ -27	-5 ~ 7	7 ~ 10
5	520	401	770	610	1	-3 ~ 0	-6 ~ 5	-1 ~ 2	-2 ~ 4
					2	-8 ~ 3	-6 ~ -4	-6 ~ 0	1 ~ 15
6	520	401	770	570	1	-8 ~ 2	-7 ~ 15	-2 ~1	-3 ~ 7
					2	-7 ~ 3	-6 ~ 0	-6 ~ 0	-1 ~ 15
7	520	401	770	670	1	-5 ~ 3	-8 ~- 6	-4 ~ -1	-1 ~ 17
					2	-10 ~ 2	-3 ~ 3	-5 ~ 1	-4 ~ 17
8	520	401	770	840	1	-3 ~ 2	-10 ~ 4	-1 ~ 0	0 ~ 7
					2	-6 ~ 2	-4 ~ 0	-4 ~ 0	0 ~ 16

a) The system includes one type of vanadium cation in the analyzed solution; b) The system includes two types of vanadium cations in the analyzed solution; c) 0.0565, 0.0848, 0.113, 0.141 and 0.17 mol dm^{-3}; d) 0.004, 0.006, 0.008, 0.01, 0.02, 0.024, 0.028, 0.032, 0.036 and 0.04 mol dm^{-3}; e) 0.024, 0.028, 0.032, 0.036 and 0.04 mol dm^{-3}; f) Additional wavelength; g) Values printed in italics are identical to the values for set 0; h) Values are rounded to the first decimal point; i) **Case 1**: V^{2+} and V^{3+}; **Case 2**: V^{2+}, V^{3+} and VO^{2+}

Table-6 demonstrates the concentration calculations of mixed solutions, which were calculated from absorption spectra (Fig. 9), at selected wavelengths using matrix F in Table-4. Table-6 shows that the formula set 0 gives relative account concentrations with errors of the sets of 0 and 5. The deviations of the concentrations for the test solutions of No. 1 are less than 10 % and there is little difference between **Case 1** and **Case 2**. In the test solution of No.2, the deviations are less than 5 %. Alternatively, by using the additional wavelength λ′ = 610 nm in set 5, the accuracy improved (Table-6).

With regard to the inverse problem, the stability of the analytical solution against the measured noise is determined by eqn. (14). Again, the value Λ is related to the molar absorption coefficients, especially in the contracted system. This means that the appropriate mixing of the spectra is required to obtain the eigenvectors with the appropriate Λ values to provide stability against possible noise or errors.

TABLE-6
COMPARISON OF CALCULATED CONCENTRATIONS OF c_n USING g_n FOR TEST SOLUTIONS WITH UNKNOWN CONCENTRATIONS. THE ABSORBANCES ARE 0.439 FOR 520 nm, 0.706 for 401 nm, 0.224 for 770 nm and 0.645 FOR 610 nm IN THE SOLUTION NO. 1 AND ARE 0.090 FOR 520 nm, 0.327 for 401 nm, 0.373 for 770 nm AND 0.348 FOR 610 nm IN SOLUTION NO. 2

No.[b)]	Case	c_n[a)] for n by set 0/mol dm^{-3}			c_n[a)] for n by set 5/mol dm^{-3}		
		1(V^{2+})	2(V^{3+})	3(VO^{2+})	1(V^{2+})	2(V^{3+})	3($V0^{2+}$)
1	1	0.11	0.035	-	0.114	0.031	-
		(0.113)	(0.032)	-	(0.113)	(0.032)	-
	dev[c)]	-2%	10%	-	1%	-3%	-
	2	0.110	0.036	-0.000	0.110	0.035	-0.000
		(0.113)	(0.032)	(0.000)	(0.113)	(0.032)	(0.000)
	dev[c)]	-3%	11%	-	-3%	9%	-
2	2	0.000	0.027	0.020	0.000	0.028	0.020
		(0.000)	(0.028)	(0.020)	(0.000)	(0.028)	(0.020)
	dev[c)]	-[d)]	-4%	0%	-	0%	0%
	3	-	0.028	0.020	-	0.028	0.022
		-	(0.028)	(0.020)	-	(0.028)	(0.020)
	dev[c)]	-	0%	0%	-	0%	8%

a) Parenthetical values are dissolved values of vanadium cation in the solutions; b) No. of test solutions; c) Deviation from the prepared concentration; d) Undefined

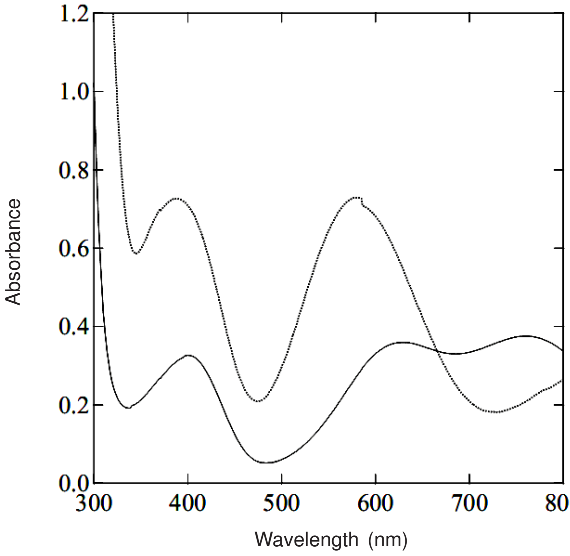

Fig. 9. Absorption spectra of test solutions No. 1 (dot line) and 2 (solid line) in 2 mol dm^{-3} H_2SO_4

Conclusion

To develop a simplified and simultaneous quantification method for vanadium ions at various oxidation states, we obtained the eigenvectors of absorption spectra and concentrations. In all of the systems (V^{2+} and V^{3+} in **Case 1**, V^{2+}, V^{3+}, and VO^{2+} in **Case 2**, V^{3+} and VO^{2+} in **Case 3**, and V^{2+}, V^{3+}, VO^{2+} and VO_2^+ in **Case 4**), the number of the eigenvectors is identical to the number of the species included. This led us to the selection of the wavelength λ for which the number of the selected wavelength is identical to the number of the species included. The result shows that the concentration was determined within an error of 5 % (10 %). This new method of analysis will provide future theoretical guidance for monitoring vanadium redox-flow batteries and will advance the practical applications and commercial success of vanadium redox-flow batteries.

ACKNOWLEDGEMENTS

The financial support of the National Basic Research Program of China (973 Program No. 2010CB227201) and the National Science Foundation Committee of China (50972165) is greatly appreciated. The present work was partially supported by a Grant-in-Aid for Scientific Research (B) 22360408 from the Japan Society for the Promotion of Science (JSPS).

REFERENCES

1. E. Sum, M. Rychcik and M. Skyllas-Kazacos, *J. Power Sour.*, **15**, 179 (1985).
2. E. Sum, M. Rychcik and M. Skyllas-Kazacos, *J. Power Sour.*, **16**, 85 (1985).
3. M. Futamata, S. Higuchi, O. Nakamura, I. Ogino, Y. Takada, S. Okazaki, S. Ashimura and S. Takahashi, *J. Power Sour.*, **24**, 137 (1988).
4. M. Skyllas-Kazacos, G. Kazacos, G. Poon and H. Verseema, *Int. J. Energy Res.*, **34**, 182 (2010).
5. N. Tokuda, T. Kanno, T. Hara, T. Sigematsu, Y. Tsutsui, A. Ikeuchi, T. Itou and T. Kumamoto, *SEI Tech. Rev.*, **50**, 88 (2000).
6. D.J. You, H.M. Zhang and J. Chen, *Electrochim. Acta*, **54**, 6827 (2009).
7. X. Wu, S. Peng, B. Feng, T. Yamamura, T. Yano, I. Satoh, S. Liu and K. Huang, *J. Inorg. Mater.*, **26**, 535 (2011).
8. M. Taylor and J. van Staden, *Analyst*, **119**, 1263 (1994).
9. J. Wei, N. Teshima and T. Sakai, *Anal. Sci.*, **24**, 371 (2008).
10. A. Safavi, M. Nezhad and E. Shams, *Anal. Chim. Acta*, **409**, 283 (2000).
11. M. Skyllas-Kazacos, C. Menictas and M. Kazakos, *J. Electrochem. Soc.*, **143**, L86 (1996).
12. C. Root, *Anal. Chem.*, **37**, 1600 (1965).
13. R. Bennett and O. Holmes, *Can. J. Chem.*, **38**, 2319 (1960).
14. B. Figgis, Introduction to Ligand Fields, Interscience Publishers, New York (1966).
15. C. Ballhausen and H. Gray, *Inorg. Chem.*, **1**, 111 (1960).
16. Y. Israel, L. Meites, in eds.: A. Bard, R. Parsons and J. Jordan, Standard Potentials in Aqueous Solution, Marcel Dekker, Inc., New York, p. 507 (1985).
17. K. Varmuza and P. Filzmoser, Introduction to Multivariate Statistical Analysis in Chemometrics, CRC Press, Boca Raton (2009).
18. T. Yamamura, X. Wu, S. Ohta, K. Shirasaki, H. Sakuraba, I. Satoh and T. Shikama, *J. Power Sour.*, **196**, 4003 (2011).
19. O. Holmes and D. McClure, *J. Chem. Phys.*, **26**, 1686 (1957).
20. C. Jørgensen, *Acta Chem. Scand.*, **11**, 73 (1957).